Molecular and Cellular Endocrinology 443 (2017) 52–62

Contents lists available at ScienceDirect

Molecular and Cellular Endocrinology

journal homepage: www.elsevier.com/locate/mce

Plasma from pre-pubertal obese children impairs insulin stimulated Nitric Oxide (NO) bioavailability in endothelial cells: Role of ER stress

Natalia Di Pietro [a, c, d, *], M. Loredana Marcovecchio [a, c, d], Sara Di Silvestre [b, c, d], Tommaso de Giorgis [a, c, d], Vincenzo Giuseppe Pio Cordone [b, c, d], Paola Lanuti [a, c, d], Francesco Chiarelli [a, c, d], Giuseppina Bologna [a, c, d], Angelika Mohn [a, c, d], Assunta Pandolfi [b, c, d]

[a] Department of Medicine and Aging Sciences, University "G. d'Annunzio", Chieti-Pescara, Italy
[b] Department of Medical, Oral and Biotechnological Sciences, University "G. d'Annunzio", Chieti-Pescara, Italy
[c] Centro Scienze dell'Invecchiamento e Medicina Traslazionale (CeSI-MeT), University "G. d'Annunzio", Chieti-Pescara, Italy
[d] "G. d'Annunzio" University Foundation, Chieti, Italy

ARTICLE INFO

Article history:
Received 14 June 2016
Received in revised form
16 November 2016
Accepted 2 January 2017
Available online 3 January 2017

Keywords:
Obesity
Endothelial dysfunction
Nitric oxide
ER stress
Insulin resistance

ABSTRACT

Childhood obesity is commonly associated with early signs of endothelial dysfunction, characterized by impairment of insulin signaling and vascular Nitric Oxide (NO) availability. However, the underlying mechanisms remain to be established. Hence, we tested the hypothesis that endothelial insulin-stimulated NO production and availability was impaired and related to Endoplasmic Reticulum (ER) in human umbilical vein endothelial cells (HUVECs) cultured with plasma obtained from pre-pubertal obese (OB) children.

OB children (N = 28, age: 8.8 ± 2.2; BMI z-score: 2.15 ± 0.39) showed impaired fasting glucose, insulin and HOMA-IR than normal weight children (CTRL; N = 28, age: 8.8 ± 1.7; BMI z-score: 0.17 ± 0.96). The *in vitro* experiments showed that OB-plasma significantly impaired endothelial insulin-stimulated NO production and bioavailability compared to CTRL-plasma. In parallel, in HUVECs OB-plasma increased GRP78 and activated PERK, eIF2α, IkBα and ATF6 (all ER stress markers). Moreover, OB-plasma increased NF-κB activation and its nuclear translocation. Notably, all these effects proved to be significantly restored by using PBA and TUDCA, known ER stress inhibitors.

Our study demonstrate for the first time that plasma from obese children is able to induce *in vitro* endothelial insulin resistance, which is characterized by reduced insulin-stimulated NO production and bioavailability, endothelial ER stress and increased NF-κB activation.

1. Introduction

Childhood obesity has reached epidemic proportions worldwide, and has become a major public health issue (Deckelbaum and Williams, 2001). There is plenty of evidence that, in conjunction with the growing epidemic of childhood obesity, cardiovascular (CV) disease is becoming more prevalent (Cote et al., 2013). Obese children are predisposed to the development of subclinical CV alterations early in life and to an increased CV morbidity and mortality in adulthood (Cote et al., 2013). Many metabolic and inflammatory factors are implicated in the pathogenesis of vascular changes in obese children (Gidding and Daniels, 2016). In particular, insulin resistance (IR) represents a key link between childhood obesity and the associated CV risk, being one of the first mechanisms involved in the development of endothelial dysfunction (Chiarelli and Marcovecchio, 2008). IR contributes to high blood pressure, dyslipidemia, liver steatosis and increased carotid intima-media thickness already in obese pre-pubertal children (D'Adamo et al., 2008; de Giorgis et al., 2014; Giannini et al., 2008; Marcovecchio et al., 2006). The presence of vascular IR can induce an imbalance between pro- and anti-atherogenic endothelial insulin signaling pathways. Such imbalance impairs endothelial Nitric Oxide (NO) Synthase (eNOS) activation and NO release and

* Corresponding author. Aging and Translational Medicine Research Center (CeSI-MeT), Room 421, "G. d'Annunzio" University Chieti-Pescara, "Gabriele d'Annunzio" University Foundation, Via Luigi Polacchi, 11, 66100 Chieti, Italy.
E-mail address: n.dipietro@unich.it (N. Di Pietro).

http://dx.doi.org/10.1016/j.mce.2017.01.001

bioavailability (Pandolfi and De Filippis, 2007; Pandolfi et al., 2005). It is known that NO, constitutively generated by endothelial cells, plays an important role in the maintenance of vascular homeostasis and in the pro-inflammatory response characterizing the early stages of atherosclerosis (Fleming, 2010). Thus, a reduction in NO bioavailability, which occurs under IR conditions (Muniyappa and Sowers, 2013), promotes inflammation. A crucial step in this process is the activation of nuclear factor kappa-light-chain-enhancer of activated B cells (NF-κB)-pathway which, in turn, contribute to endothelial dysfunction in the early stage of atherosclerosis, by increasing the expression of adhesion molecules such as vascular and intercellular cell adhesion molecules (VCAM and ICAM) (Di Tomo et al., 2012).

Recently, Endoplasmic Reticulum (ER) stress has been linked to vascular dysfunction (Cimellaro et al., 2016; Galan et al., 2014; Lenna et al., 2014; Sozen et al., 2015) in the context of obesity and IR (Leiria et al., 2013; Ozcan et al., 2004; Salvado et al., 2015; Zhang et al., 2013; Zhou et al., 2012). One of the key roles of the ER is to ensure proper synthesis, folding and transport of proteins (Mollereau et al., 2014; Walter and Ron, 2011). When the ER becomes stressed due to the accumulation of newly synthesized unfolded/misfolded proteins, unfolded protein response (UPR) is activated. UPR is mediated by ER transmembrane receptor proteins which are inositol-requiring kinase 1 (IRE1), double-stranded RNA-activated protein kinase-like endoplasmic reticulum kinase (PERK) and activating transcription factor 6 (ATF6) (Walter and Ron, 2011). As a starting signal for UPR, misfolded proteins induce release of glucose-regulated protein 78 (GRP78, also called BiP) from these transmembrane stress sensors and therefore enhance their activation. Once activated: (i) IRE1 receptor, by its endoribonuclease activity, cleaves a 26 base-pair segment from the mRNA of the X-box binding protein-1 (XBP1), creating an alternative message that is translated into the active (or spliced) form of the transcription factor (XBP1s); (ii) by phosphorylation, PERK activates eukaryotic translation initiation factor 2 alpha (eIF2α); (iii) the third branch of UPR requires translocation of ATF6 to the Golgi apparatus where it is cleaved to produce an active transcription factor (Hotamisligil, 2010).

The severity and duration of the stress response are crucial in determining the cell fate between survival and death, mild and/or acute ER stress generally resulting in adaptation and severe and/or chronic ER stress resulting in cellular dysfunction and/or cell apoptosis (Mollereau et al., 2014).

Recent findings have shown that ER stress and UPR pathways link to major inflammatory and stress signaling networks, including activation of NF-κB- inhibitor α (IkBα)- pathways (IKK), as well as production of ROS (Gotoh and Mori, 2006; Hotamisligil, 2010; Nakajima and Kitamura, 2013; Tam et al., 2012). Interestingly, UPR has also been related to obesity-associated IR in peripheral organs such as the liver (Ozcan et al., 2004). Based on such evidence, we hypothesized that in pre-pubertal obese children ER stress might play a crucial role in modulating NO endothelial bioavailability through regulation of insulin signaling.

Up to now, only a few studies have investigated NO bioavailability in obese pre-pubertal children and adolescents (Codoner-Franch et al., 2011; Gruber et al., 2008) suggesting impaired NO bioavailability in obese youth, but the cellular mechanisms underlying NO regulation and the potential involvement of ER stress have not been investigated yet.

In the present study, we demonstrate that in human umbilical vein endothelial cells (HUVECs) plasma from obese children is able to induce endothelial ER stress and this is associated with increased inflammation and reduced insulin-stimulated NO production and bioavailability. Furthermore, we found that inhibition of ER stress significantly improves vascular insulin resistance *in vitro*, suggesting that new mechanisms are potentially involved in childhood obesity-related vascular dysfunction.

2. Materials and methods

2.1. Study population

Plasma was obtained from 28 obese and 28 normal-weight prepubertal children. Obese children were recruited from patients attending the Pediatric Endocrinology Clinic of the Department of Pediatrics, University of Chieti, Italy. The study protocol was approved by the Ethics Committee of the University of Chieti, and, in adherence with the Declaration of Helsinki, written informed consent was obtained from all subjects taking part in the study.

All subjects were obese (BMI>95th percentile for age and sex), but otherwise healthy. None had other chronic diseases (diabetes, endocrine disorders, hereditary diseases, or systemic inflammation) or were taking any medication. The control group was recruited from children attending the Pediatric outpatient clinics for a general check 1–2 weeks after a previous admission to our Pediatric ward for minor diseases (mainly gastroenteritis and trauma). At the time of assessment, these children were in good general health with complete resolution of the original disease. The inclusion criteria of the control group were: normal weight (BMI between 5 and 85th for age and sex), being otherwise in good health and not having any chronic disease. None of the patients was taking any medication and none had a history of smoking or alcohol consumption.

All children underwent a complete physical examination, including anthropometric measurements (height, weight, BMI). Fasting blood samples were collected to measure glucose and insulin levels and for the *in vitro* studies. The Homeostasis Model Assessment of insulin resistance (HOMA-IR) was used as a surrogate index of insulin resistance and it was calculated as: [fasting insulin (mU/l) × fasting glucose (mmol/l)/22.5] (Matthews et al., 1985).

2.2. Anthropometric measurements

Body weight was determined to the nearest 0.1 kg, and height was measured by Harpenden stadiometer to the nearest 0.1 cm. BMI and WC were used as indexes of adiposity. BMI was calculated as the weight in kilograms divided by the square of the height in meters and was converted into standard deviation scores (SDS) using published reference values for age and sex for the Italian population (Cacciari et al., 2006).

2.3. Biochemical analysis

Serum glucose levels were determined using the glucose oxidase method, and serum insulin levels were measured by the two-site immunoenzymetric assay (AIA-PACK IRI; Tosoh, Tokyo, Japan).

2.4. Plasma collection

At the time of blood collection all subjects were fasting and free of common infectious diseases. Blood was drawn by venipuncture into evacuated tubes containing ethylenediaminetetraacetic acid (EDTA). In order to obtain the plasmatic fraction, the whole blood was centrifuged at 1578 *g* for 10 min room temperature, the separated plasma was stored at −80 °C until experimental analysis.

2.5. Antibodies and materials

M199 endothelial growth medium, DMEM, glutamine,

phosphate buffered saline (PBS), 0.05% trypsin/0.02% EDTA, Thapsigargin (Thaps), N-nitro l-arginine methyl ester (L-NAME, LN), 1 H-oxadiazole-[4,3-alpha]-quinoxalin-1-one (ODQ), Tauroursodeoxycholic acid (TUDCA), Tris/HCl, EDTA and Dowex AGWX8-200 were from Sigma Chemicals (St.Louis, MO, USA). Fetal Bovine Serum (FBS) was purchased from GIBCO-Life-Technologies (Monza, Italy) and tissue-culture disposables were from Eppendorf (Hamburg, Germany). Anti-eNOS and anti-phosphorylated-eNOS (Serine 1177) antibodies were from BD Biosciences (Becton Dickinson, Milan, Italy) while antibodies, anti-protein kinase B (Akt), anti-phosphorylated-Akt (Serine 473), anti-glucose-regulated protein-78 kDa (GRP78), protein kinase RNA-like endoplasmic reticulum kinase (PERK), phosphorylated-PERK (p-PERK), eukaryotic translation initiation factor-2alpha (eIF2α), phosphorylated-eIF2α (p-eIF2α), X-box binding protein-1 spliced (XBP1s), nuclear factor of kappa light polypeptide gene enhancer in B-cells inhibitor-alpha (IkBα), phosphorylated-kBα (p-IkBα) and nuclear factor kappa-light-chain-enhancer of activated B cells (NF-κB) were from Cell Signaling Technology (Beverly, MA, USA). Tunicamycin (Tunica), activating transcription factor-6 (ATF6 cleaved and not cleaved), inositol-requiring enzyme-1 (IRE1) and phosphorylated-IRE1 (p-IRE1) antibodies were from Abcam (Cambridge, UK). Anti-β-actin mouse monoclonal antibody was from Sigma Aldrich (St. Louis, MO, USA). For flow cytometry, FITC-labeled secondary antibodies were from thermo-fisher (Milan, Italy) and DRAQ-5 was from Biostatus (UK). 4-Phenylbutyric acid (PBA) was from Calbiochem (Italy). L-(3H)-arginine was purchased from PerkinElmer Italia S. p.a. (Milan, Italy).

2.6. Cell cultures

Umbilical cords were obtained from randomly selected healthy Caucasian mothers delivering at the Hospital of Chieti and Pescara. All procedures were in agreement with the ethical standards of the Institutional Committee on Human Experimentation and with the Declaration of Helsinki Principles. After approval of the protocol by the Institutional Review Board, signed informed consent was obtained from each participating subject. Primary HUVECs were obtained as described previously and used between the 3rd and 5th passages *in vitro* (Di Fulvio et al., 2014). In this study, fifteen different HUVEC batches were employed and each experiment was performed on cells coming at least from three different batches.

2.7. Experimental protocols

In order to assess the NOS activity and cGMP levels HUVECs were serum starved for 16 h and then grown for 24 h with 10% plasma obtained from OB- (plasma OB, N = 13) or CTRL-children (plasma CTRL, N = 13) or with 10% FBS (as Basal control) in the presence or absence of insulin (Ins,100 nM). In some experiments 2 μM of ionomycin (Ion, positive control), 1 mM of L-NAME (LN, selective inhibitor of NO synthase activity) and 10 μM ODQ (heme-site inhibitor of soluble guanylyl cyclase competitive with NO) were also employed. Moreover, in order to evaluate the possible involvement of ER stress, in some other experiments 5 mM PBA or 500 μM TUDCA (ER stress inhibitors) was pre-incubated for 1 h and left for the last 24 h.

In order to investigate the effect of plasma OB on Akt and eNOS phosphorylation levels and the possible involvement of ER stress, quiescent HUVECs (16 h starvation) were pretreated or not for 1 h with PBA (10 mM) and TUDCA (1 mM, ER stress inhibitor), then incubated for 3 h with Thaps (1 μM) or Tunica (1 μM, both ER stress inducers) in baseline condition, or with 10% FBS (as Basal control) and a 10% of three different plasma pool (each pool with six OB- or CTRL-plasmas) while insulin (100 mM) was added for 15 min.

To thoroughly evaluate ER stress marker induction (Oslowski and Urano, 2011) (GRP78, PERK, eIF2α, ATF6, IRE1, XBP1s and IkBα) and NF-κB activation and nuclear translocation, HUVECs were treated as described above, following a temporary (3hrs, also called early induction, see eNOS phosphorylation experimental protocol above) or chronic (24hrs, also called late induction, see NOS activity and cGMP levels experimental protocol above) incubation with OB- and CTRL-plasmas or FBS (Basal Control).

It is important to specify that plasma was used both individually and in a pool of six plasmas. The pool of six OB- or CTRL-plasmas was used because of the difficulty in obtaining an adequate amount of blood from children.

2.8. NOS activity by conversion of L-[^{3}H]-arginine into L-[^{3}H]-citrulline

Insulin-stimulated NOS activity was evaluated in HUVECs cultured with 10% plasma obtained from OB- (N = 13) or CTRL-children (N = 13) as described in the experimental protocol by measuring the conversion of L-[3H]-arginine into L-[3H]-citrulline as previously described (Di Pietro et al., 2006).

2.9. Intracellular cGMP determination

Since increased/decreased NO synthesis does not necessarily translate into increased/decreased NO bioavailability, we measured the intracellular cGMP levels, a good proxy for NO in the vasculature which ought to reflect the bioavailable NO. Intracellular cGMP levels were evaluated in HUVECs cultured with 10% plasma obtained from OB- (N = 13) or CTRL-children (N = 13) as described in the experimental protocol using a commercially available Enzyme Immunoassay (EIA) kit (GE Healthcare, Little Chalfont, Buckinghamshire, UK) following the manufacturer's instructions.

2.10. Flow cytometry

ER stress and inflammatory pathways were determined in HUVECs cultured with 10% plasma obtained from OB- (N = 13) or CTRL-children (N = 13) or with a pool of six OB- or CTRL-plasmas as described in the experimental protocol by flow cytometry or imaging flow cytometry analysis performed as previously reported (Lanuti et al., 2016). Briefly, samples were fixed and permeabilized by using the IntraSure Kit (BD Biosciences), as suggested by the manufacturer's instructions. Cells were, then stained by primary antibodies against markers of vascular insulin signaling (mouse anti-eNOS, mouse anti-phospho-Ser^{1177}eNOS, rabbit anti-Akt and anti-phospho-Ser^{473}Akt), ER stress (rabbit anti-GRP78, rabbit anti-PERK, rabbit anti-p-PERK, mouse anti-eIF2α, rabbit anti-p-eIF2α, mouse anti-ATF6, rabbit anti-IRE1, rabbit anti-p-IRE1 and rabbit anti-XBP1s) and vascular inflammatory markers (mouse anti-IkBα, mouse anti-p-IkBα, rabbit anti-NF-κB). The incubation of primary antibody was followed by incubation with the specific FITC-labeled secondary antibody. For some experiments, the nucleus was stained with Biostatus-DRAQ5.

For flow cytometry, cells were analyzed on a FACS Canto II flow cytometer (BD Biosciences), using CellQuest™ software 3.2.1. f1 (BD) (Lanuti et al., 2006). Quality control included a regular check-up with Cytometer Setup and Tracking (CS&T) beads (BD Biosciences). Debris was excluded from the analysis by gating on morphological parameters; 10,000 non-debris events in the morphological gate were recorded for each sample. All antibodies were titrated under assay conditions and optimal photomultiplier (PMT) gains were established for each channel. Data were analyzed using FlowJo™ v.8.8.6 software (TreeStar, Ashland, OR). The Mean Fluorescence Intensity Ratio (MFI Ratio) was calculated dividing the

MFI of positive events by the MFI of negative events.

For imaging flow cytometry sample acquisitions were performed by ImageStream (Amnis, Seattle, WA, USA; one laser, six-color configuration) (Bologna et al., 2014). To assess unspecific fluorescence, samples were stained with the respective secondary antibody alone. Analyses were performed by IDEAS software (Amnis). Data were indicated as a percentage of the markers mentioned above positive cells in live cells either permeabilized or not.

2.11. Statistical analysis

All data were expressed as means ± SD or median [interquartile range], unless otherwise stated. Not normally distributed variables were log transformed before data analysis. Differences between the two study groups in continuous variables were tested by unpaired *t*-test. For *in vitro* studies, differences were assessed by the Student *t*-test and by ANOVA test. P values < 0.05 were considered statistically significant.

3. Results

3.1. Clinical and metabolic characteristics

Table 1 shows the general characteristics of the study population which included 28 obese (OB) and 28 normal-weight (CTRL) children. The two groups were comparable for age, whereas, as expected, weight, BMI and BMI z-score were higher in obese than control children. Fasting glucose, insulin and HOMA-IR were significantly higher in obese than in control children.

3.2. Basal and stimulated NO production

We first assessed whether plasma from OB-children might impair the NO production in insulin-stimulated HUVECs as compared to cells incubated with plasma from CTRL-children. As shown in Fig. 1, in cells treated for 24 h with 10% OB-plasma insulin was unable to increase NO release which, on the contrary, significantly increased in HUVECs treated with 10% CTRL-plasma. Pre-incubation with L-NAME, a known NOS inhibitor, significantly reduced insulin-stimulated NO production. In addition, to test the hypothesis that ER stress might trigger endothelial IR, HUVECs were pre-incubated with PBA (5 mM), a chemical chaperone that is known to reduce ER stress *in vitro* and *in vivo* (Oslowski and Urano, 2011). Interestingly, PBA significantly restored insulin-mediated NO production in endothelial cells cultured with OB-plasma and the use of L-NAME significantly abolished this effect. In the same experimental condition, HUVECs were stimulated by ionomycin, a calcium ionophore that induces NO production mainly via mobilization of intracellular Ca^{2+}. Differently from the result obtained following insulin stimulation, NO release was significantly increased by ionomycin compared to the basal condition and pre-treatment with L-NAME totally abolished this effect. This result suggests that in HUVECs the role of OB-plasma in reducing insulin stimulated NO production was specific. .

In order to assess the integrity of eNOS activation system, HUVECs were cultured both under normal growth conditions (10% FBS) and CTRL-plasma and then exposed to insulin or ionomycin. In these conditions, insulin- and ionomycin-stimulated endothelial NO production proved to be both increased while pretreatment with L-NAME completely abolished these effects.

Table 1
Clinical and biochemical characteristics of the study population.

	Obese children	Control children	P value
N	28	28	
Age (years)	8.8 ± 2.2	8.8 ± 1.7	0.94
Height (cm)	135.8 ± 11.4	126.0 ± 10.7	0.003
Weight (Kg)	50.9 ± 10.1	26.3 ± 9.3	<0.001
BMI (Kg/m^2)	27.4 ± 2.9	17.4 ± 3.0	<0.001
BMI z-score	2.15 ± 0.39	0.17 ± 0.96	<0.001
Glycemia (mg/dl)	87.5 ± 8.9	79.4 ± 7.0	0.001
Insulin (mU/ml)	15.0 [11.4–22.1]	6.2 [5.2–7.3]	<0.001
HOMA	3.3 [2.5–4.2]	1.2 [1.1–1.4]	<0.001

Data are mean ± SD or median [25th-75th percentile].

3.3. Basal and stimulated cGMP levels

We next investigated whether endothelial cells treated with OB- or CTRL-plasma were able to generate insulin-stimulated bioactive NO. For this purpose, we measured the formation of cGMP, a good proxy for NO, because soluble guanylate cyclase is activated by nanomolar concentrations of the gas (Bulotta et al., 2001; Di Tomo et al., 2012).

As shown in Fig. 2, exposure to insulin resulted in a significant increase in cGMP over controls in HUVECs treated for 24 h both with 10% FBS and with CTRL-plasma, which were both inhibited by the presence of L-NAME. On the contrary, insulin was unable to increase cGMP levels when HUVECs were cultured for 24 h with 10% OB-plasma. Notably, pre-incubation of HUVECs with PBA significantly reversed this phenomenon, indicating that this may be associated with ER stress and the use of L-NAME significantly abolished this effect. HUVECs under normal growth conditions (10% FBS) or incubated with 10% CTRL- or OB-plasma were also stimulated with ionomycin which significantly increased cGMP levels in all conditions. In the same experimental settings, pre-incubation with L-NAME significantly abolished these effects. Furthermore, in order to discriminate between cGMP-dependent and cGMP-independent NO effects, the ODQ (heme-site inhibitor of soluble guanylyl cyclase competitive with NO) was used. This GC-inhibitor significantly abolished the insulin and ionomycin effects, suggesting a NO-activation of guanylyl cyclase.

3.4. Effect of ER stress on insulin-stimulated Akt and eNOS phosphorylation

We then evaluated whether OB-plasma might impair insulin-stimulated Akt and eNOS activation by phosphorylation. First, we evaluated the phosphorylation levels in Serine 473 of Akt, which is a known upstream regulator of eNOS in the insulin-signalling cascade. Incubation of HUVECs with OB-plasma significantly decreased the insulin−stimulated Akt phosphorylation levels (2 folds *vs* Basal condition $p < 0.05$) while in normal growth condition and in cells incubated with CTRL-plasma Akt phosphorylation levels was increased (2.5 folds and 2.2 folds *vs* Basal condition $p < 0.05$, respectively).

Then, we focused on eNOS activation, the pivotal enzyme in the endothelial NO production. As shown in Fig. 3, exposure to insulin significantly increased phospho-Ser^{1177}eNOS levels over controls in HUVECs treated for 3 h both with 10% FBS and with 10% CTRL-plasmas (three different pool of six different CTRL-plasma). On the contrary, insulin was not able to increase eNOS phosphorylation levels following incubation with 10% OB-plasma (three different pool of six different OB-plasmas). Interestingly, this result was reversed after pre-incubation of HUVECs with known ER stress inhibitors (Oslowski and Urano, 2011) such as PBA or TUDCA, proving the involvement of ER stress. By way of experimental control, HUVECs under normal growth conditions (10% FBS) were also stimulated for 3hrs with thapsigargin or tunicamycin, a known inducers of ER stress (Oslowski and Urano, 2011). Notably,

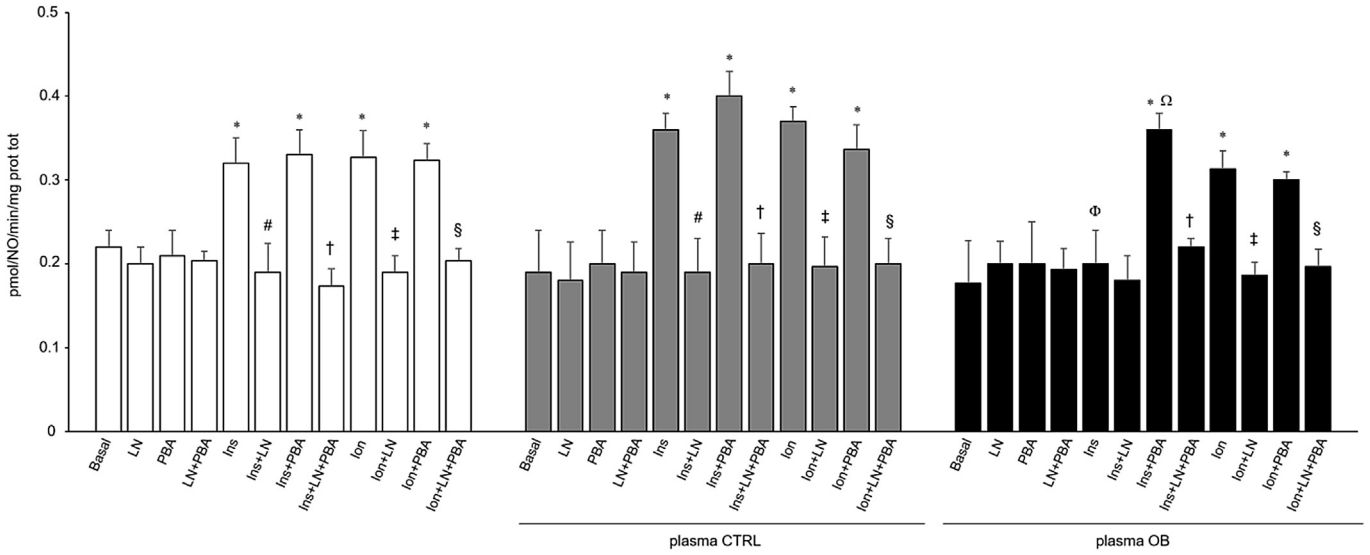

Fig. 1. Basal and stimulated NO production. HUVECs serum starved were incubated for 24 h with plasma obtained from OB- (plasma OB, N = 13) or CTRL-children (plasma CTRL, N = 13) or with 10% FBS (as Basal control). Insulin (Ins), Ionomycin (Ion), L-NAME (LN) and PBA were also employed. NOS activity was determined by the conversion of L-[3H]-arginine into L-[3H]-citrulline and expressed as pmol/NO/min/mg prot tot. Data were expressed as means ± SD of at least six different experiments. $^{*}p < 0.02$ *vs* Basal; $^{\#}p < 0.02$ *vs* Ins; $^{\dagger}p < 0.009$ *vs* Ins+PBA; $^{\ddagger}p < 0.004$ *vs* Ion; $^{\S}p < 0.005$ *vs* Ion+PBA; $^{\Phi}p < 0.02$ *vs* Ins baseline and Ins plasma CTRL; $^{\Omega}p < 0.02$ *vs* Ins plasma OB.

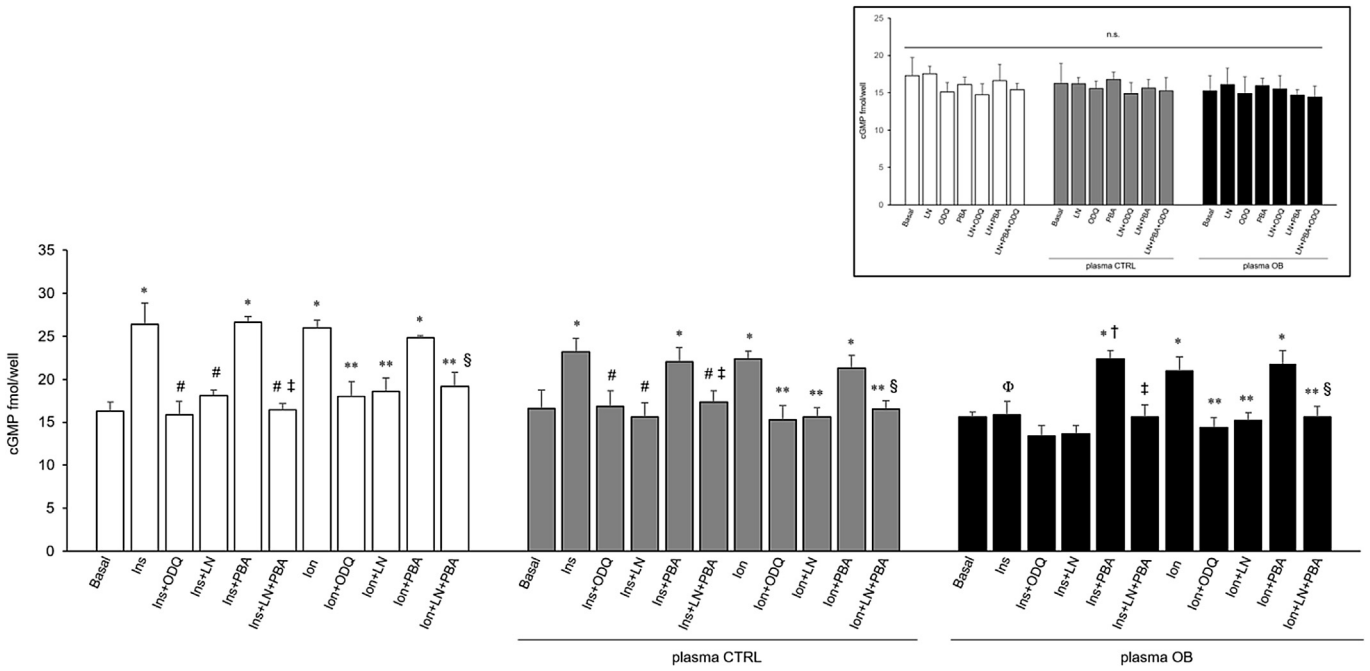

Fig. 2. Basal and stimulated cGMP levels. HUVECs serum starved were incubated for 24 h with 10% OB- (N = 10) or CTRL-plasma (N = 10) or with 10% FBS (Basal control). Insulin (Ins), Ionomycin (Ion), ODQ, L-NAME (LN) and PBA were also employed. The inset shows the effect of ODQ, LN and PBA by themselves or in association on unstimulated HUVECs. Intracellular cGMP levels are expressed as mean of cGMP fmol/well ±SD of at least six different experiments. $^{*}p < 0.02$ *vs* Basal; $^{\#}p < 0.02$ *vs* Ins; $^{\ddagger}p < 0.01$ *vs* Ins+PBA; $^{**}p < 0.02$ *vs* Ion; $^{\S}p < 0.01$ *vs* Ion+PBA; $^{\Phi}p < 0.005$ *vs* Ins baseline and Ins plasma CTRL; $^{\dagger}p < 0.004$ *vs* Ins plasma OB; no significant (n.s.).

tunicamycin significantly decreased endothelial eNOS phosphorylation levels compared to basal condition while, as expected, pre-incubation with either PBA or TUDCA restored the levels to baseline. In addition, tunicamycin significantly inhibited insulin-stimulated eNOS phosphorylation, indicating that induction of ER stress might be relevant to inducing IR in vascular endothelial cells. On the contrary, the stimulation with thapsigargin significantly increased the phospho-Ser^{1177}eNOS levels. This is not surprising considering that, although the thapsigargin is considered an ER stress inducer, it is also known as an agonist of the calcium-mediated activation of eNOS.

3.5. ER stress marker induction

Since we found a potential ER stress involvement in the impaired endothelial insulin-stimulated NO bioavailability triggered by OB-plasma, we next focused on evaluation of the main ER stress markers. In particular, we first evaluated the effect of OB-

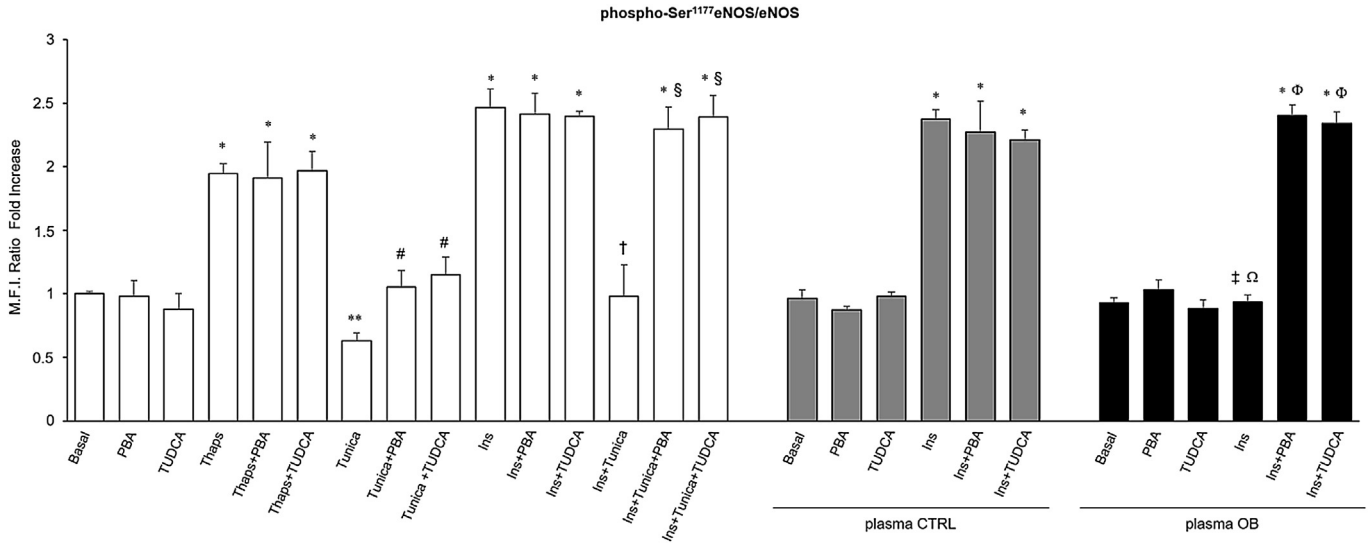

Fig. 3. Effect of ER stress on basal and insulin-stimulated eNOS phosphorylation levels. HUVECs serum starved were pretreated or not with PBA or TUDCA, following 3 h stimulation with: Thapsigargin (Thaps), Tunicamycin (Tunica), 10% FBS (Basal control) and 10% pool of six OB- or CTRL-plasmas. In some experiments insulin (Ins) was employed. Data were expressed as phospho-Ser^{1177}eNOS on total eNOS fold increase ± SD (at least three different experiments) of Mean Fluorescence Intensity Ratio (M.F.I Ratio) versus Basal condition. M.F.I. Ratio was calculated dividing the M.F.I. of positive events by the M.F.I. of negative events. $^{*}p < 0.001$ *vs* Basal; $^{**}p < 0.002$ *vs* Basal; $^{\#}p < 0.007$ *vs* Tunica; $^{\dagger}p < 0.001$ *vs* Ins; $^{\S}p < 0.002$ *vs* Ins+Tunica; $^{\ddagger}p < 0.001$ *vs* Ins Basal; $^{\Omega}p < 0.001$ *vs* Ins plasma CTRL; $^{\Phi}p < 0.001$ *vs* Ins plasma OB.

plasma on early and late induction of the three main ER transmembrane receptor proteins (PERK, IRE1 and ATF6) and their upstream regulator GRP78.

Incubation of HUVECs for 3 h (Fig. 4A–D) with 10% OB-plasma (pool of six different OB-plasmas) significantly increased GRP78, PERK phosphorylation, cleaved ATF6 levels and ATF6 nuclear translocation (Fig. 5) as compared to incubation with 10% CTRL-plasma (pool of six different CTRL-plasmas) or to basal condition (10% FBS), while IRE1 proved not to be activated. The same results were achieved after 24 h (Fig. 4E–H) incubation of HUVECs with 10% OB- or CTRL-plasma and 10% FBS. Meanwhile, in the same experimental conditions, neither CTRL-plasma nor FBS (basal condition) affected the expression of ER stress markers (Fig. 4A–H). As a positive control, endothelial cells grown under normal conditions (10% FBS) were also treated with thapsigargin for 3 h (1 μM, Fig. 4A–D) or 24 h (20 nM, Fig. 4E–H). As expected, all the above-mentioned ER stress markers proved significantly increased.

After measuring the activation of the three master regulators of UPR, we focused on the potential activation of some downstream effectors such as eIF2α, IkBα and XBP1s.

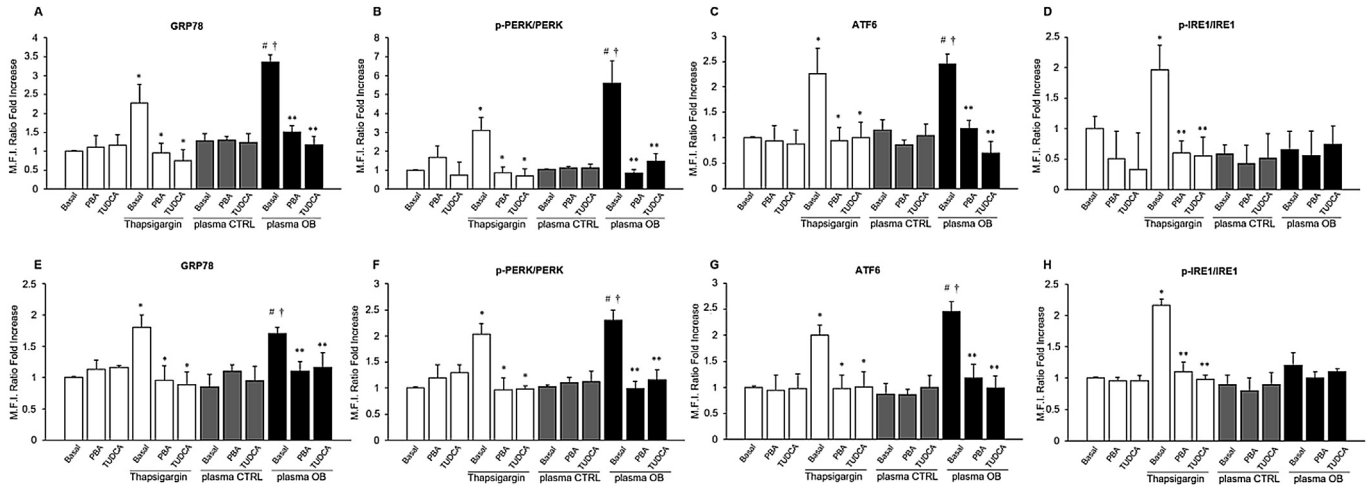

Fig. 4. Early and late induction of ER stress markers. (*A-D*) HUVECs serum starved were pretreated or not with PBA or TUDCA, following 3 h incubation with: Thapsigargin (Thaps), 10% FBS (Basal control) and 10% pool of six OB- or CTRL-plasmas. (*E-H*) HUVECs serum starved were pretreated or not with PBA or TUDCA, following 24 h incubation with: 10% OB- (N = 10) or CTRL-plasma (N = 10), Thapsigargin (Thaps) or with 10% FBS (Basal control). (*A-H*) All ER stress markers were expressed as fold increase ± SD (at least three different experiments) of Mean Fluorescence Intensity Ratio (M.F.I Ratio) *versus* Basal condition. M.F.I. Ratio was calculated dividing the M.F.I. of positive events by the M.F.I. of negative events. (*A*) GRP78 levels ($^{*}p < 0.02$ *vs* Basal and *vs* Basal Thaps; $^{\#}p < 0.001$ *vs* Basal; $^{\dagger}p < 0.002$ *vs* plasma CTRL; $^{**}p < 0.002$ *vs* Basal plasma OB); (*B*) PERK and p-PERK, data expressed as ratio of p-PERK on total PERK levels ($^{*}p < 0.008$ *vs* Basal and *vs* Basal Thaps; $^{\#}p < 0.003$ *vs* Basal; $^{\dagger}p < 0.003$ *vs* Basal plasma CTRL; $^{**}p < 0.003$ *vs* Basal plasma OB); (*C*) ATF6 levels ($^{*}p < 0.02$ *vs* Basal and *vs* Basal Thaps; $^{\#}p < 0.001$ *vs* Basal; $^{\dagger}p < 0.002$ *vs* Basal plasma CTRL; $^{**}p < 0.002$ *vs* Basal plasma OB); (*D*) IRE1 and p-IRE1, data expressed as ratio of p-IRE1 on total IRE1 levels ($^{*}p < 0.002$ *vs* Basal; $^{**}p < 0.02$ *vs* Basal Thaps); (*E*) GRP78 levels ($^{*}p < 0.009$ *vs* Basal and *vs* Basal Thaps; $^{\#}p < 0.0003$ *vs* Basal; $^{\dagger}p < 0.003$ *vs* Basal plasma CTRL; $^{**}p < 0.02$ *vs* Basal plasma OB); (*F*) PERK and p-PERK, data expressed as ratio of p-PERK on total PERK levels ($^{*}p < 0.004$ *vs* Basal and *vs* Basal Thaps; $^{\#}p < 0.0004$ *vs* Basal; $^{\dagger}p < 0.0005$ *vs* Basal plasma CTRL; $^{**}p < 0.002$ *vs* Basal plasma OB); (G) ATF6 levels ($^{*}p < 0.009$ *vs* Basal and *vs* Basal Thaps; $^{\#}p < 0.0003$ *vs* Basal; $^{\dagger}p < 0.0007$ *vs* Basal plasma CTRL; $^{**}p < 0.003$ *vs* Basal plasma OB); (*H*) IRE1 and p-IRE1, data expressed as ratio of p-IRE1 on total IRE1 levels ($^{*}p < 0.0001$ *vs* Basal; $^{**}p < 0.0006$ *vs* Basal Thaps).

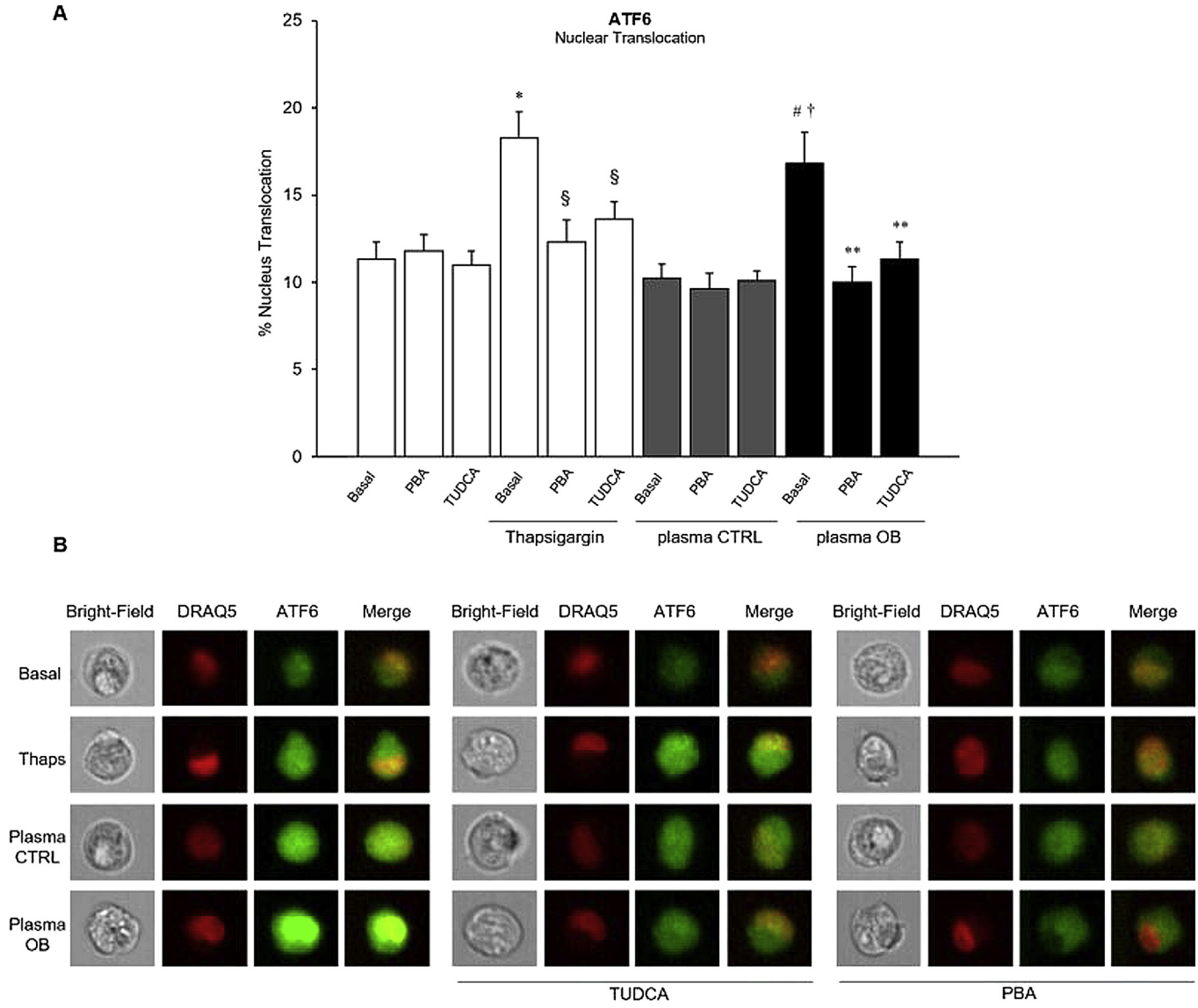

Fig. 5. ATF6 nuclear translocation. HUVECs serum starved were pretreated or not with PBA or TUDCA, following 3 h incubation with: Thapsigargin (Thaps), 10% FBS (Basal control) and 10% pool of six OB- or CTRL-plasmas. (*A*) ATF6 nuclear translocation was indicated as mean of the percentage of ATF6 positive cells in live cells ± SD ($^{*}p < 0.003$ *vs* Basal; $^{§}p < 0.02$ *vs* Basal Thaps; $^{\#}p < 0.01$ *vs* Basal; $^{\dagger}p < 0.02$ *vs* Basal plasma CTRL; $^{**}p < 0.009$ *vs* Basal plasma OB); (*B*) Representative single cell images of ATF6 cytoplasm-nucleus translocation in the absence (left panel) or in the presence of TUDCA (central panel) or PBA (right panel).

HUVECs incubation with 10% OB-plasma for 24 h significantly increased eIF2α and IkBα (Fig. 6A and B, respectively) phosphorylation levels, whereas, as expected, the spliced form of XBP1, XBP1s (Fig. 6C), was not increased. In the same experimental condition ER stress markers were unaffected by CTRL-plasma treatment, while thapsigargin (20 nM) significantly increased eIF2α, IkBα and XBP1s.

All the ER stress markers triggered by thapsigargin were reduced when HUVECs were pre-incubated with TUDCA and PBA (Figs. 4–6).

3.6. NF-κB activation

We next demonstrated that incubation for 24 h with 10% plasma from OB children triggered a significant increase in NF-κB activation in HUVECs as compared to plasma from CTRL children (Fig. 7A). Interestingly, OB-plasma also increased NF-κB nuclear translocation significantly more than did CTRL-plasma (Fig. 7B and C). Meanwhile, under the same experimental conditions, neither CTRL-plasma nor 10% FBS affected the NF-κB expression and nuclear translocation (Fig. 7A and B-C, respectively).

The effect of incubation with thapsigargin (20 nM) for 24 h on endothelial cells at baseline was also evaluated, demonstrating an increase in both NF-κB activation and translocation (Fig. 7A and B-C, respectively). These data may suggest that, in our cellular model, apart from conventional inflammatory activation, ER stress also takes part in NF-κB activation. Interestingly, the enhanced endothelial NF-κB activation triggered by OB-plasma was significantly reduced following pre-incubation with PBA and TUDCA (Fig. 7A). These two ER stress inhibitors were also significantly effective in inhibiting NF-κB nuclear translocation (Fig. 7B and C). We did not observe any changes in the activation of NF-κB in HUVECs grown under normal conditions (10% FBS) and incubated with ER stress inhibitors (Fig. 7A–C).

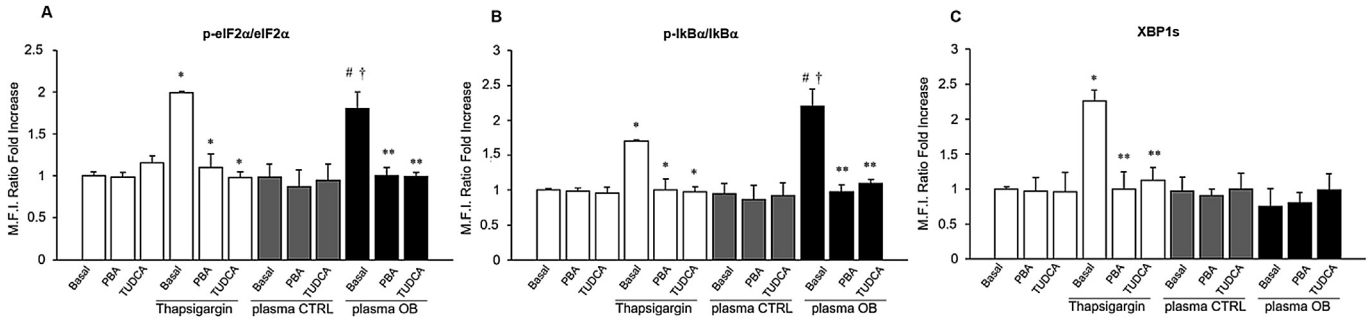

Fig. 6. Downstream ER stress and inflammatory markers activation. HUVECs serum starved were pre-treated or not with PBA or TUDCA, following 24 h incubation with: 10% OB- (N = 10) or CTRL-plasma (N = 10), Thapsigargin (Thaps) or with 10% FBS (Basal control). (*A-C*) All ER stress markers were expressed as fold increase ± SD (at least three different experiments) of Mean Fluorescence Intensity Ratio (M.F.I Ratio) *versus* Basal condition. M.F.I. Ratio was calculated dividing the M.F.I. of positive events by the M.F.I. of negative events. (*A*) eIF2α and p-eIF2α, data expressed as ratio of p-eIF2α on total eIF2α levels ($^{*}p < 0.0006$ *vs* Basal and *vs* Basal Thaps; $^{\#}p < 0.002$ *vs* Basal; $^{\dagger}p < 0.005$ *vs* Basal plasma CTRL; $^{**}p < 0.003$ *vs* Basal plasma OB); (*B*) IkBα and p-IkBα, data expressed as ratio of p-IkBα on total IkBα levels ($^{*}p < 0.001$ *vs* Basal and *vs* Basal Thaps; $^{\#}p < 0.001$ *vs* Basal; $^{\dagger}p < 0.002$ *vs* Basal plasma CTRL; $^{**}p < 0.002$ *vs* Basal plasma OB); (*C*) XBP1s levels ($^{*}p < 0.0001$ *vs* Basal; $^{**}p < 0.002$ *vs* Basal Thaps).

4. Discussion

Childhood obesity is commonly associated with early signs of endothelial dysfunction, characterized by impairment of insulin signaling, vascular NO availability and increased inflammation (Chiarelli and Marcovecchio, 2008; Giannini et al., 2008; Marcovecchio et al., 2006). Recently all these features have been associated with ER stress (Flamment et al., 2012; Gotoh et al., 2011; Lenna et al., 2014; Ozcan et al., 2004) and some recent studies have also investigated the underlying mechanisms (Galan et al., 2014; Gotoh and Mori, 2006; Leiria et al., 2013; Sozen et al., 2015; Tam et al., 2012; Yang et al., 2015; Zeng et al., 2014; Zhang et al., 2013;

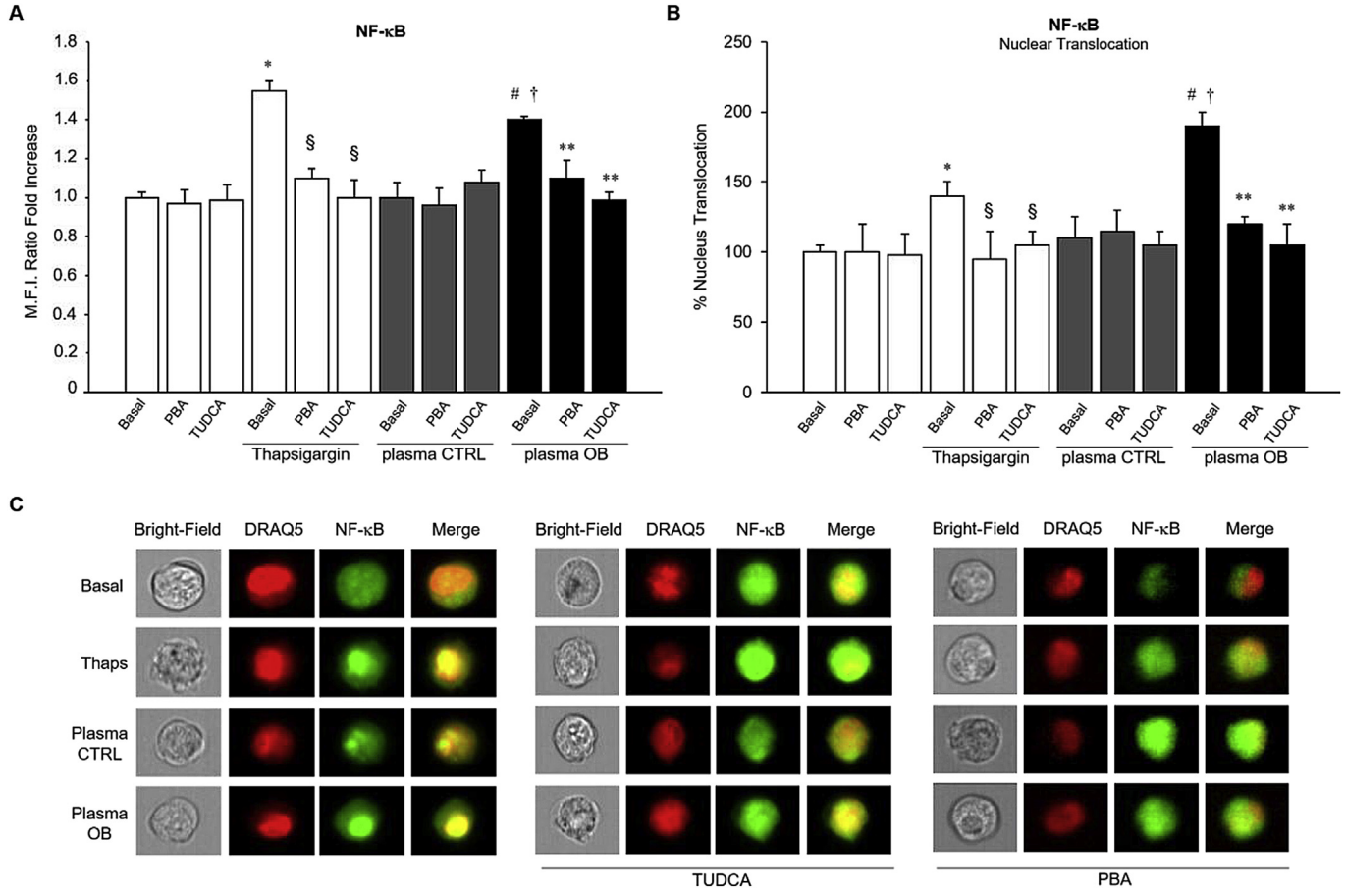

Fig. 7. NF-κB activation and nuclear translocation. HUVECs serum starved were pretreated or not with PBA or TUDCA, following 24 h incubation with: 10% OB- (N = 10) or CTRL-plasma (N = 10), Thapsigargin (Thaps) or with 10% FBS (Basal control). (*A*) NF-κB levels were expressed as Fold increase ± SD (at least three different experiments) of Mean Fluorescence Intensity Ratio (M.F.I Ratio) *versus* Basal condition. M.F.I. Ratio was calculated dividing the M.F.I. of positive events by the M.F.I. of negative events ($^{*}p < 0.007$ *vs* Basal and *vs* Basal Thaps; $^{\#}p < 0.002$ *vs* Basal; $^{\dagger}p < 0.001$ *vs* Basal plasma CTRL; $^{**}p < 0.003$ *vs* Basal plasma OB); (*B*) NF-κB nuclear translocation was indicated as mean of the percentage of NF-κB positive cells in live cells ± SD ($^{*}p < 0.005$ *vs* Basal, $^{\#}p < 0.02$ *vs* Basal plasma CTRL, $^{\dagger}p < 0.008$ *vs* Basal, $^{**}p < 0.002$ *vs* Basal plasma OB); (*C*) Representative single cell images of NF-κB cytoplasm-nucleus translocation in the absence (left panel) or in the presence of TUDCA (central panel) or PBA (right panel).

Zhou et al., 2012), although much still remains to be explored.

In particular, up to now there have been no findings regarding the role of ER stress in the mechanism/s leading to vascular dysfunction in the context of childhood obesity.

Hence, in the present study, for the first time, we showed that plasma from pre-pubertal obese children impairs insulin-stimulated NO production and bioavailability in endothelial cells. Moreover, this is associated with increased ER stress induction, given the increased levels of the main ER stress markers (GRP78, PERK, ATF6, eIF2α and IkBα) and, in parallel, increased NF-κB activation, a known key component of the inflammatory response. Interestingly, inhibition of ER stress, by chemical chaperones such as PBA and TUDCA, ameliorates plasma OB-induced insulin resistance and inflammation in HUVECs.

Hitherto only a few *in vivo* studies have investigated NO bioavailability in obese pre-pubertal children and adolescents (Codoner-Franch et al., 2011; Gruber et al., 2008). Gruber and colleagues (Gruber et al., 2008) suggested that juvenile (about 14 years of age) obesity might contribute to atherogenesis via reduced NO bioavailability. More recently, Codoner-Franch et al. (2011). reported increased plasma levels of nitrite and nitrate, suggesting increased nitrosative stress in severely obese children aged between 7 and 14 years. Although the above-mentioned studies agree in indicating impaired NO bioavailability in obese youth, studies are lacking on the mechanisms potentially involved in endothelial NO bioavailability impairment relating to an IR condition in childhood.

Here, employing the innovative system of studying plasma from obese children, we proved that such plasma induced insulin resistance in cultured vascular endothelial cells. Thus, as compared to plasma CTRL and basal condition, insulin stimulation failed to induce an increase in NO production, bioavailability, eNOS and Akt phosphorylation following incubation with plasma OB. It is interesting to note that all these effects were reversed after HUVEC incubation with ER stress inhibitors (PBA or TUDCA), suggesting that the induction of ER stress is implicated in the vascular insulin resistance triggered by plasma OB.

This result agrees with recent findings by Galan et al. (2014), who showed that endothelial cells stimulated with tunicamycin decreased the expression of active eNOS while this effect was restored by using PBA or TUDCA.

Several lines of evidence suggest that ER stress is a potential mechanism involved in both insulin resistance and endothelial dysfunction (Flamment et al., 2012; Galan et al., 2014; Gotoh and Mori, 2006, 2011; Leiria et al., 2013; Lenna et al., 2014; Ozcan et al., 2004; Sozen et al., 2015; Zeng et al., 2014; Zhang et al., 2013; Zhou et al., 2012). In particular, in line with our findings, Zhou et al. (2012). have recently demonstrated that insulin-stimulated eNOS activity, NO release and eNOS phosphorylation were impaired in vascular endothelial cells and related to ER stress following incubation with serum from patients with chronic kidney disease (CKD). Note that, as observed in our study, incubation with ER stress inhibitors (PBA or TUDCA) annulled the inhibitory effect triggered by CKD-serum.

In our study, once we had found that use of ER stress inhibitors improved OB-plasma impaired vascular insulin sensitivity, we looked more deeply at the effect of such plasma on unfolded protein response activation.

Here we noted that OB-plasma caused a significant increase in ER stress upstream regulators GRP78, followed by activation of two of the three main ER transmembrane receptor proteins PERK and ATF6, while IRE1 and downstream XBP1 were not activated following 3, 24 h (Fig. 4) and 1 h stimulation (data not shown).

In this regard, although it is known that the UPR is generally driven by the activation of all three ER-localized transmembrane signal transducers, recently several studies have reported possible distinct involvement of the three UPR branches in metabolically active tissues (Cimellaro et al., 2016; Kaplon et al., 2013; Puri et al., 2008).

Furthermore, by evaluating eIF2α and IkBα activation, which are downstream ER stress effectors of PERK, they both proved significantly increased following OB-plasma incubation. In parallel, OB-plasma triggered a significant increase in NF-κB activation and its nuclear translocation in endothelial cells.

Recent findings have shown that ER stress and UPR pathways connect with major inflammatory and stress signaling networks, including activation of the IkBα pathway as well as production of ROS and NO (Gotoh and Mori, 2006; Hotamisligil, 2010; Nakajima and Kitamura, 2013; Tam et al., 2012).

In line with these findings, in our cellular model PBA and TUDCA significantly restores to basal condition both NF-κB activation and nuclear translocation (Fig. 5). These data indicate that, conventional activation apart, this transcription factor might be a consequence of ER stress as also reported by other authors (Tam et al., 2012; Zeng et al., 2014). In this regard, it has been shown that PERK mediates the release of NF-κB from its inhibitor IκB and consequently, by its nuclear-translocation, leads to expression of a variety of different genes involved in inflammatory pathways (Hotamisligil, 2010). In parallel, the ATF6 pathway has likewise been shown to directly activate NF-κB (Hotamisligil, 2010).

More recently, Tam and colleagues (Tam et al., 2012) reported a novel involvement of both PERK and IRE1 in the activation of NF-κB. However, since IRE1 was not activated in our cellular model, we suppose that NF-κB activation may be mainly linked to PERK-mediated phosphorylation of eIF2α as previously reported by other authors (Jiang et al., 2003). Furthermore, one might consider that PERK could potentially represent an important crossroads between inflammation and insulin resistance. In this connection, it has recently been reported that inhibition of PERK improves cellular insulin responsiveness at the level of FOXO activity (Zhang et al., 2013).

In addition, although the molecular mechanism linking ER stress and its effect on vascular insulin resistance remains unclear, a potential role has been proposed for tribbles homolog 3 (TRIB3). TRIB3 is a pseudo-kinase inhibitor of AKT, which is the direct upstream activator of eNOS (Prudente et al., 2012) and has been shown to be relevant to insulin resistance (Bromati et al., 2011; Leiria et al., 2013). Furthermore, TRIB3 has also been linked to ER stress-induced insulin resistance in skeletal muscle from high-fat diet-induced insulin resistant mice (Koh et al., 2013) as well as to β-cell apoptosis via NF-κB pathway activation (Fang et al., 2014). Thus, a possible role by TRIB3 in the impaired insulin response triggered by plasma OB in our cellular model might be hypothesized.

In addition, we have previously demonstrated that plasma from obese children shows increased circulating inflammatory and oxidative stress markers (sensitive C-reactive protein [hs-CRP] and urinary isoprostanes [PGF-2α], respectively) (Giannini et al., 2008) which are known to promote the early stage of atherogenesis. Thus, one might hypothesize that these plasma biochemical alterations may induce *in vitro* the impairment of several insulin stimulated endothelial functions demonstrated in our cellular model.

Moreover, circulating microRNAs (miRNAs), a novel group of non-coding small RNAs, have been found to be dysregulated in metabolic diseases, such as obesity, type 2 diabetes and atherosclerosis (Vienberg et al., 2016). One notes that they have recently been linked to the unfolded protein response pathways in relation to various physiological processes. Since it has recently been demonstrated that changes in circulating miRNAs are also associated with childhood obesity (Carolan et al., 2014; Prats-Puig et al., 2013), one might also speculate that they contribute to the

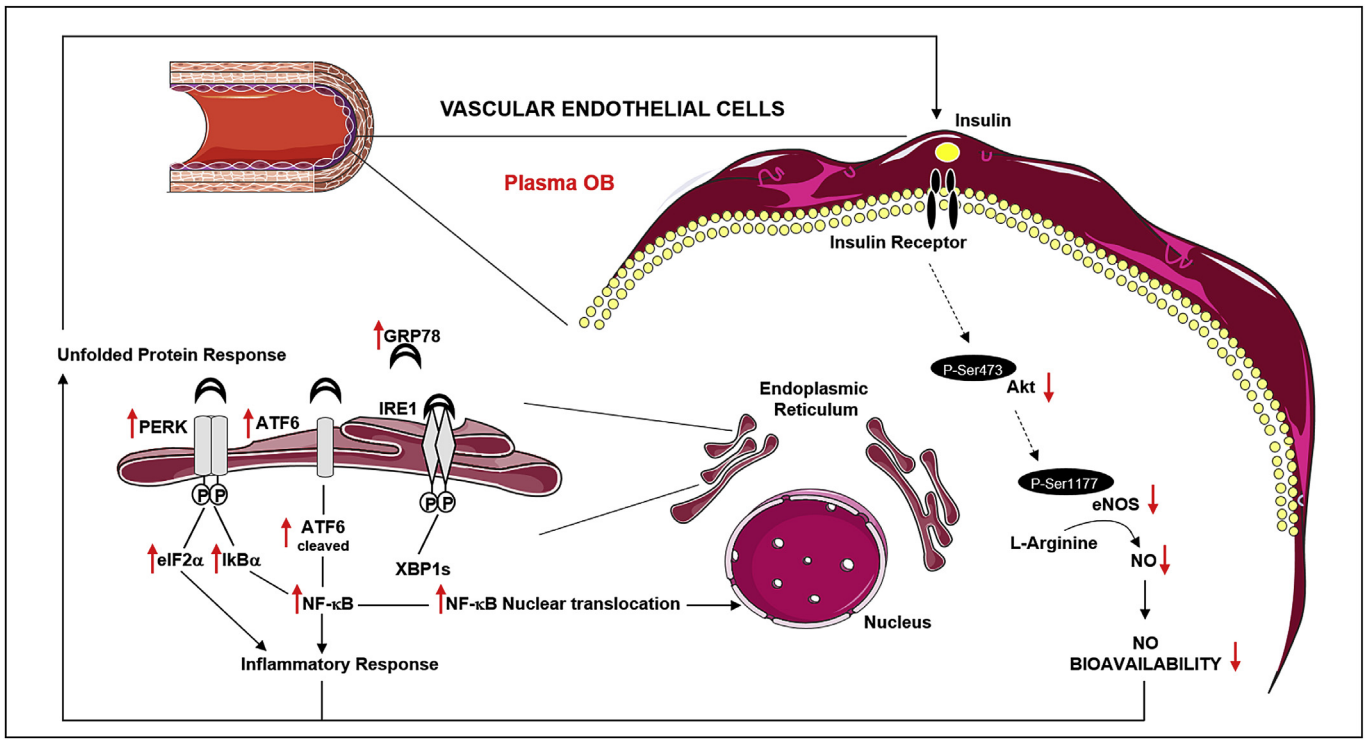

Fig. 8. Effect of plasma from obese children on vascular endothelial cells. As summarized in this scheme plasma from severely obese children (Plasma OB) affect endothelial function by acting on several intracellular signaling pathways. First, a reduced insulin sensitivity leads to decreased Akt and eNOS activation by phosphorylation and consequently reduction of insulin-stimulated NO production and bioavailability, which, as well known, might contribute to endothelial dysfunction. Secondly, increased Endoplasmic Reticulum (ER) stress activation leads to the induction of the Unfolded Protein Response (UPR) pathway. In particular GRP78 (ER stress upstream regulator), PERK and ATF6 (both ER stress transmembrane sensor proteins), eIF2α and ATF6 cleaved (both downstream ER stress markers) and IkBα (ER stress and Inflammatory marker) result all increased, while IRE1 results not involved in this process. In parallel, the induction of these pathways lead to increase NF-κB activation, thus resulting in increased inflammatory response. In addition, it should be emphasized that a mutual interaction probably exists between factors that cause ER stress and factors that are generated by ER stress. Thus, a vicious circle triggered by OB plasma may contribute to endothelial dysfunction. Nitric Oxide (NO), endothelial Nitric Oxide Synthase (eNOS), protein kinase B (known as Akt), glucose-regulated protein 78 (GRP78, also called BiP), inositol-requiring kinase 1 (IRE1), double-stranded RNA-activated protein kinase-like endoplasmic reticulum kinase (PERK), activating transcription factor 6 (ATF6), eukaryotic translation initiation factor 2 alpha (eIF2α), nuclear factor of kappa light polypeptide gene enhancer in B-cells inhibitor, alpha (IkBα), X-box binding protein-1 spilced (XBP1s), nuclear factor kappa-light-chain-enhancer of activated B cells (NF-κB).

mechanism causing ER stress induction in vascular cells. In this regard, it has recently emerged that miRNAs are key regulators of ER stress homeostasis and important players in UPR – dependent signaling (Maurel and Chevet, 2013).

Taking these findings all together, it is clear that the molecular mechanisms linking ER stress to insulin resistance in vascular endothelial cells are numerous and require further study.

However, we believe that our study does add some key understanding of the deleterious effects that obesity may have on the vasculature right from childhood, particularly in relation to the induction of endothelial dysfunction.

In summary (Fig. 8), our study provides the first evidence that plasma from pre-pubertal obese children reduces insulin-stimulated NO production and bioavailability in endothelial cells, which, in turn might contribute to endothelial dysfunction. Furthermore, the present study highlights the involvement of ER stress in this process, which in turn also increases the endothelial inflammatory response. Although a deeper study of the underlying mechanisms is necessary, our study could contribute to the development of new preventive and therapeutic strategies aiming to reduce the early onset of vascular complications even in childhood.

Funding sources

This study was supported in part by a grant from the Italian Ministry of Education, University and Research (MIUR): PRIN 201098WFZ2_007.

Conflict of interest

None declared.

References

Bologna, G., Lanuti, P., D'Ambrosio, P., Tonucci, L., Pierdomenico, L., D'Emilio, C., Celli, N., Marchisio, M., d'Alessandro, N., Santavenere, E., Bressan, M., Miscia, S., 2014. Water-soluble platinum phthalocyanines as potential antitumor agents. Biometals 27, 575–589.

Bromati, C.R., Lellis-Santos, C., Yamanaka, T.S., Nogueira, T.C., Leonelli, M., Caperuto, L.C., Gorjao, R., Leite, A.R., Anhe, G.F., Bordin, S., 2011. UPR induces transient burst of apoptosis in islets of early lactating rats through reduced AKT phosphorylation via ATF4/CHOP stimulation of TRB3 expression. Am. J. Physiol. Regul. Integr. Comp. Physiol. 300, R92–R100.

Bulotta, S., Barsacchi, R., Rotiroti, D., Borgese, N., Clementi, E., 2001. Activation of the endothelial nitric-oxide synthase by tumor necrosis factor-alpha. A novel feedback mechanism regulating cell death. J. Biol. Chem. 276, 6529–6536.

Cacciari, E., Milani, S., Balsamo, A., Spada, E., Bona, G., Cavallo, L., Cerutti, F., Gargantini, L., Greggio, N., Tonini, G., Cicognani, A., 2006. Italian cross-sectional growth charts for height, weight and BMI (2 to 20 yr). J. Endocrinol. Invest. 29, 581–593.

Carolan, E., Hogan, A.E., Corrigan, M., Gaotswe, G., O'Connell, J., Foley, N., O'Neill, L.A., Cody, D., O'Shea, D., 2014. The impact of childhood obesity on inflammation, innate immune cell frequency, and metabolic microRNA expression. J. Clin. Endocrinol. Metab. 99, E474–E478.

Chiarelli, F., Marcovecchio, M.L., 2008. Insulin resistance and obesity in childhood. Eur. J. Endocrinol. 1 (159 Suppl. l), S67–S74.

Cimellaro, A., Perticone, M., Fiorentino, T.V., Sciacqua, A., Hribal, M.L., 2016. Role of

endoplasmic reticulum stress in endothelial dysfunction. Nutr. Metab. Cardiovasc Dis. 26, 863–871.
Codoner-Franch, P., Tavarez-Alonso, S., Murria-Estal, R., Megias-Vericat, J., Tortajada-Girbes, M., Alonso-Iglesias, E., 2011. Nitric oxide production is increased in severely obese children and related to markers of oxidative stress and inflammation. Atherosclerosis 215, 475–480.
Cote, A.T., Harris, K.C., Panagiotopoulos, C., Sandor, G.G., Devlin, A.M., 2013. Childhood obesity and cardiovascular dysfunction. J. Am. Coll. Cardiol. 62, 1309–1319.
D'Adamo, E., Impicciatore, M., Capanna, R., Loredana Marcovecchio, M., Masuccio, F.G., Chiarelli, F., Mohn, A.A., 2008. Liver steatosis in obese prepubertal children: a possible role of insulin resistance. Obes. (Silver Spring) 16, 677–683.
de Giorgis, T., Marcovecchio, M.L., Di Giovanni, I., Giannini, C., Chiavaroli, V., Chiarelli, F., Mohn, A., 2014. Triglycerides-to-HDL ratio as a new marker of endothelial dysfunction in obese prepubertal children. Eur. J. Endocrinol. 170, 173–180.
Deckelbaum, R.J., Williams, C.L., 2001. Childhood obesity: the health issue. Obes. Res. 4 (9 Suppl. l), 239S–243S.
Di Fulvio, P., Pandolfi, A., Formoso, G., Di Silvestre, S., Di Tomo, P., Giardinelli, A., De Marco, A., Di Pietro, N., Taraborrelli, M., Sancilio, S., Di Pietro, R., Piantelli, M., Consoli, A., 2014. Features of endothelial dysfunction in umbilical cord vessels of women with gestational diabetes. Nutr. Metab. Cardiovasc Dis. 24, 1337–1345.
Di Pietro, R., Mariggio, M.A., Guarnieri, S., Sancilio, S., Giardinelli, A., Di Silvestre, S., Consoli, A., Zauli, G., Pandolfi, A., 2006. Tumor necrosis factor-related apoptosis-inducing ligand (TRAIL) regulates endothelial nitric oxide synthase (eNOS) activity and its localization within the human vein endothelial cells (HUVEC) in culture. J. Cell Biochem. 97, 782–794.
Di Tomo, P., Canali, R., Ciavardelli, D., Di Silvestre, S., De Marco, A., Giardinelli, A., Pipino, C., Di Pietro, N., Virgili, F., Pandolfi, A., 2012. beta-Carotene and lycopene affect endothelial response to TNF-alpha reducing nitro-oxidative stress and interaction with monocytes. Mol. Nutr. Food Res. 56, 217–227.
Fang, N., Zhang, W., Xu, S., Lin, H., Wang, Z., Liu, H., Fang, Q., Li, C., Peng, L., Lou, J., 2014. TRIB3 alters endoplasmic reticulum stress-induced beta-cell apoptosis via the NF-kappaB pathway. Metabolism 63, 822–830.
Flamment, M., Hajduch, E., Ferre, P., Foufelle, F., 2012. New insights into ER stress-induced insulin resistance. Trends Endocrinol. Metab. 23, 381–390.
Fleming, I., 2010. Molecular mechanisms underlying the activation of eNOS. Pflugers Arch. 459, 793–806.
Galan, M., Kassan, M., Kadowitz, P.J., Trebak, M., Belmadani, S., Matrougui, K., 2014. Mechanism of endoplasmic reticulum stress-induced vascular endothelial dysfunction. Biochim. Biophys. Acta 1843, 1063–1075.
Giannini, C., de Giorgis, T., Scarinci, A., Ciampani, M., Marcovecchio, M.L., Chiarelli, F., Mohn, A., 2008. Obese related effects of inflammatory markers and insulin resistance on increased carotid intima media thickness in pre-pubertal children. Atherosclerosis 197, 448–456.
Gidding, S.S., Daniels, S.R., 2016. Obesity, vascular changes, and the development of atherosclerosis. J. Pediatr. 168, 5–6.
Gotoh, T., Mori, M., 2006. Nitric oxide and endoplasmic reticulum stress. Arterioscler. Thromb. Vasc. Biol. 26, 1439–1446.
Gotoh, T., Endo, M., Oike, Y., 2011. Endoplasmic reticulum stress-related inflammation and cardiovascular diseases. Int. J. Inflam. 2011, 259462.
Gruber, H.J., Mayer, C., Mangge, H., Fauler, G., Grandits, N., Wilders-Truschnig, M., 2008. Obesity reduces the bioavailability of nitric oxide in juveniles. Int. J. Obes. (Lond) 32, 826–831.
Hotamisligil, G.S., 2010. Endoplasmic reticulum stress and the inflammatory basis of metabolic disease. Cell. 140, 900–917.
Jiang, H.Y., Wek, S.A., McGrath, B.C., Scheuner, D., Kaufman, R.J., Cavener, D.R., Wek, R.C., 2003. Phosphorylation of the alpha subunit of eukaryotic initiation factor 2 is required for activation of NF-kappaB in response to diverse cellular stresses. Mol. Cell Biol. 23, 5651–5663.
Kaplon, R.E., Chung, E., Reese, L., Cox-York, K., Seals, D.R., Gentile, C.L., 2013. Activation of the unfolded protein response in vascular endothelial cells of nondiabetic obese adults. J. Clin. Endocrinol. Metab. 98, E1505–E1509.
Koh, H.J., Toyoda, T., Didesch, M.M., Lee, M.Y., Sleeman, M.W., Kulkarni, R.N., Musi, N., Hirshman, M.F., Goodyear, L.J., 2013. Tribbles 3 mediates endoplasmic reticulum stress-induced insulin resistance in skeletal muscle. Nat. Commun. 4, 1871.
Lanuti, P., Marchisio, M., Cantilena, S., Paludi, M., Bascelli, A., Gaspari, A.R., Grifone, G., Centurione, M.A., Papa, S., Di Pietro, R., Cataldi, A., Miscia, S., Bertagnolo, V., 2006. A flow cytometry procedure for simultaneous characterization of cell DNA content and expression of intracellular protein kinase C-zeta. J. Immunol. Methods 315, 37–48.
Lanuti, P., Rotta, G., Almici, C., Avvisati, G., Budillon, A., Doretto, P., Malara, N., Marini, M., Neva, A., Simeone, P., Di Gennaro, E., Leone, A., Falda, A., Tozzoli, R., Gregorj, C., Di Cerbo, M., Trunzo, V., Mollace, V., Marchisio, M., Miscia, S., 2016. Endothelial progenitor cells, defined by the simultaneous surface expression of VEGFR2 and CD133, are not detectable in healthy peripheral and cord blood. Cytom. A 89, 259–270.
Leiria, L.O., Sollon, C., Bau, F.R., Monica, F.Z., D'Ancona, C.L., De Nucci, G., Grant, A.D., Anhe, G.F., Antunes, E., 2013. Insulin relaxes bladder via PI3K/AKT/eNOS pathway activation in mucosa: unfolded protein response-dependent insulin resistance as a cause of obesity-associated overactive bladder. J. Physiol. 591, 2259–2273.
Lenna, S., Han, R., Trojanowska, M., 2014. Endoplasmic reticulum stress and endothelial dysfunction. IUBMB Life 66, 530–537.
Marcovecchio, M.L., Patricelli, L., Zito, M., Capanna, R., Ciampani, M., Chiarelli, F., Mohn, A., 2006. Ambulatory blood pressure monitoring in obese children: role of insulin resistance. J. Hypertens. 24, 2431–2436.
Matthews, D.R., Hosker, J.P., Rudenski, A.S., Naylor, B.A., Treacher, D.F., Turner, R.C., 1985. Homeostasis model assessment: insulin resistance and beta-cell function from fasting plasma glucose and insulin concentrations in man. Diabetologia 28, 412–419.
Maurel, M., Chevet, E., 2013. Endoplasmic reticulum stress signaling: the microRNA connection. Am. J. Physiol. Cell Physiol. 304, C1117–C1126.
Mollereau, B., Manie, S., Napoletano, F., 2014. Getting the better of ER stress. J. Cell Commun. Signal 8, 311–321.
Muniyappa, R., Sowers, J.R., 2013. Role of insulin resistance in endothelial dysfunction. Rev. Endocr. Metab. Disord. 14, 5–12.
Nakajima, S., Kitamura, M., 2013. Bidirectional regulation of NF-kappaB by reactive oxygen species: a role of unfolded protein response. Free Radic. Biol. Med. 65, 162–174.
Oslowski, C.M., Urano, F., 2011. Measuring ER stress and the unfolded protein response using mammalian tissue culture system. Methods Enzymol. 490, 71–92.
Ozcan, U., Cao, Q., Yilmaz, E., Lee, A.H., Iwakoshi, N.N., Ozdelen, E., Tuncman, G., Gorgun, C., Glimcher, L.H., Hotamisligil, G.S., 2004. Endoplasmic reticulum stress links obesity, insulin action, and type 2 diabetes. Science 306, 457–461.
Pandolfi, A., De Filippis, E.A., 2007. Chronic hyperglicemia and nitric oxide bioavailability play a pivotal role in pro-atherogenic vascular modifications. Genes Nutr. 2, 195–208.
Pandolfi, A., Solini, A., Pellegrini, G., Mincione, G., Di Silvestre, S., Chiozzi, P., Giardinelli, A., Di Marcantonio, M.C., Piccirelli, A., Capani, F., Consoli, A., 2005. Selective insulin resistance affecting nitric oxide release but not plasminogen activator inhibitor-1 synthesis in fibroblasts from insulin-resistant individuals. Arterioscler. Thromb. Vasc. Biol. 25, 2392–2397.
Prats-Puig, A., Ortega, F.J., Mercader, J.M., Moreno-Navarrete, J.M., Moreno, M., Bonet, N., Ricart, W., Lopez-Bermejo, A., Fernandez-Real, J.M., 2013. Changes in circulating microRNAs are associated with childhood obesity. J. Clin. Endocrinol. Metab. 98, E1655–E1660.
Prudente, S., Sesti, G., Pandolfi, A., Andreozzi, F., Consoli, A., Trischitta, V., 2012. The mammalian tribbles homolog TRIB3, glucose homeostasis, and cardiovascular diseases. Endocr. Rev. 33, 526–546.
Puri, P., Mirshahi, F., Cheung, O., Natarajan, R., Maher, J.W., Kellum, J.M., Sanyal, A.J., 2008. Activation and dysregulation of the unfolded protein response in nonalcoholic fatty liver disease. Gastroenterology 134, 568–576.
Salvado, L., Palomer, X., Barroso, E., Vazquez-Carrera, M., 2015. Targeting endoplasmic reticulum stress in insulin resistance. Trends Endocrinol. Metab. 26, 438–448.
Sozen, E., Karademir, B., Ozer, N.K., 2015. Basic mechanisms in endoplasmic reticulum stress and relation to cardiovascular diseases. Free Radic. Biol. Med. 78, 30–41.
Tam, A.B., Mercado, E.L., Hoffmann, A., Niwa, M., 2012. ER stress activates NF-kappaB by integrating functions of basal IKK activity, IRE1 and PERK. PLoS One 7, e45078.
Vienberg, S., Geiger, J., Madsen, S., Dalgaard, L.T., 2016. MicroRNAs in metabolism. Acta Physiol. (Oxf) 1–16.
Walter, P., Ron, D., 2011. The unfolded protein response: from stress pathway to homeostatic regulation. Science 334, 1081–1086.
Yang, L., Calay, E.S., Fan, J., Arduini, A., Kunz, R.C., Gygi, S.P., Yalcin, A., Fu, S., Hotamisligil, G.S., 2015. METABOLISM. S-Nitrosylation links obesity-associated inflammation to endoplasmic reticulum dysfunction. Science 349, 500–506.
Zeng, W., Guo, Y.H., Qi, W., Chen, J.G., Yang, L.L., Luo, Z.F., Mu, J., Feng, B., 2014. 4-Phenylbutyric acid suppresses inflammation through regulation of endoplasmic reticulum stress of endothelial cells stimulated by uremic serum. Life Sci. 103, 15–24.
Zhang, W., Hietakangas, V., Wee, S., Lim, S.C., Gunaratne, J., Cohen, S.M., 2013. ER stress potentiates insulin resistance through PERK-mediated FOXO phosphorylation. Genes Dev. 27, 441–449.
Zhou, Q.G., Fu, X.J., Xu, G.Y., Cao, W., Liu, H.F., Nie, J., Liang, M., Hou, F.F., 2012. Vascular insulin resistance related to endoplasmic reticulum stress in aortas from a rat model of chronic kidney disease. Am. J. Physiol. Heart Circ. Physiol. 303, H1154–H1165.